Molecular Psychiatry (2005) 10, 985–997

www.nature.com/mp

ORIGINAL RESEARCH ARTICLE

SC35 promotes sustainable stress-induced alternative splicing of neuronal acetylcholinesterase mRNA

E Meshorer[1], B Bryk[1,4], D Toiber[1], J Cohen[1,2], E Podoly[1,3], A Dori[2] and H Soreq[1]

[1]*Department of Biological Chemistry, The Hebrew University of Jerusalem, Jerusalem, Israel;* [2]*Department of Neurology, Soroka University Medical Center, Beer-Sheva, Israel;* [3]*The Wolfson Centre for Structural Biology, The Hebrew University of Jerusalem, Jerusalem, Israel*

Long-lasting alternative splicing of neuronal acetylcholinesterase (AChE) pre-mRNA occurs during neuronal development and following stress, altering synaptic properties. To explore the corresponding molecular events, we sought to identify mRNAs encoding for abundant splicing factors in the prefrontal cortex (PFC) following stress. Here we show elevated levels of the splicing factor SC35 in stressed as compared with naïve mice. In cotransfections of COS-1 and HEK293 cells with an AChE minigene allowing 3′ splice variations, SC35 facilitated a shift from the primary AChE-S to the stress-induced AChE-R variant, while ASF/SF2 caused the opposite effect. Transfection with chimeric constructs comprising of SC35 and ASF/SF2 RRM/RS domains identified the SC35 RRM as responsible for AChE mRNA's alternative splicing. In poststress PFC neurons, increased SC35 mRNA and protein levels coincided with selective increase in AChE-R mRNA. In the developing mouse embryo, cortical progenitor cells in the ventricular zone displayed transient SC35 elevation concomitant with dominance of AChE-R over AChE-S mRNA. Finally, transgenic mice overexpressing human AChE-R, but not those overexpressing AChE-S, showed significant elevation in neuronal SC35 levels, suggesting a reciprocal reinforcement process. Together, these findings point to an interactive relationship of SC35 with cholinergic signals in the long-lasting consequences of stress on nervous system plasticity and development.
Molecular Psychiatry (2005) **10,** 985–997. doi:10.1038/sj.mp.4001735; published online 25 August 2005

Keywords: SC35; stress; acetylcholinesterase; alternative splicing; ASF/SF2

Long-lasting changes in alternative splicing in the nervous system[1,2] are associated with disease,[3] aging and trauma,[4] as well as with cortical neurogenesis.[5] In rats, both adult and prenatal stress reduce learning performance,[6] suggesting, among other possibilities, parallel stress-induced changes in alternative splicing. However, the molecular mechanisms leading to such changes are still largely obscure. Missplicing events are particularly prominent in human diseases.[7–9] For example, impaired splicing patterns of the glutamate transporter gene EAAT2 is associated with sporadic amyotrophic lateral sclerosis (ALS).[10] Changes in nitric oxide synthase (NOS) mRNA splicing was also reported in reactive astrocytes in the same disease.[11] This suggests plausible involvement of components of the basic splicing machinery, such as SR protein splicing factors, in ALS and other splicing-associated diseases.

Both stress and neurogenesis involve extended overexpression phases of AChE-R, the stress-associated splice variant of the acetylcholine hydrolyzing enzyme, acetylcholinesterase (AChE).[12,13] The stress- and development-associated modulations in AChE gene expression involve facilitated transcription, altered promoter usage, modified splicing patterns of the 3′ variants of the AChE pre-mRNA, and increased stability of the normally rare and unstable AChE-R mRNA transcript.[12,14] This renders AChE pre-mRNA processing an appropriate model system for exploring the involvement of alternative splicing modulations in the delayed effects of acute stress in the adult and developing brain.

Splicing alterations likely involve changes in members of the serine-arginine (SR) rich proteins, implicated in alternative splicing and splice site selection.[15] SR proteins comprise of a structurally and functionally related family, involved in multiple steps of both constitutive and alternative splicing. SR proteins, like other eukaryotic proteins binding single-stranded RNA, include one or more copies of an RNA-binding domain of about 90 amino acids, known as RNA recognition motif (RRM).[16] The RRM

Correspondence: Current address: E Meshorer, National Cancer Institute, National Institutes of Health, 41 Library Dr, Bethesda, MD 20892, USA. E-mail: meshoree@mail.nih.gov or H Soreq, Department of Biological Chemistry, The Hebrew University of Jerusalem, Jerusalem, Israel. E-mail: soreq@cc.huji.ac.il

[4]Current address: EMBL Heidelberg, Meyerhofstrasse 1, Heidelberg D-69117, Germany.

Received 12 April 2005; revised 14 July 2005; accepted 19 July 2005; published online 23 August 2005

structure consists of four strands and two helices arranged in an alpha/beta sandwich, with a third helix present during RNA binding in some cases.[17] Also, characteristic of SR proteins are modular structures with a conserved C-terminal arginine/serine-rich domain (RS domain) that interacts with components of the basic splicing machinery.[15]

The RRMs recognize weakly conserved RNA sequences, identified as either exonic or intronic splicing enhancers (ESE/ISE) or suppressors (ESS/ISS).[18] *In vivo*, the fine-tuned balance between SR-proteins, heterogeneous nuclear ribonucleic protein particles (hnRNPs), splice sites and enhancer/silencer elements is likely to be subject to modulations leading to changes in the exon usage of pre-mRNA. The levels of both SR-proteins and hnRNPs vary among tissues[19] and can be further modulated by protein phosphorylation, leading to their release from intranuclear storage compartments, such as the speckle domains at the nuclear internal boundaries.[20,21] Tissue-specific factors, especially in the nervous system, also modify these levels.[3]

Among the major SR proteins, ASF/SF2 contributes to 5′ splice site selection, through protein–protein interactions involving the RS domain,[22] whereas SC35 is required for formation of the earliest ATP-dependent splicing complex with the U1 and U2 snRNPs and the pre-mRNA. SC35 also interacts, via its RS domain, with spliceosomal components bound to both the 5′ and 3′ splice sites during spliceosome assembly. This forms a bridge between the 5′ and 3′ splice site binding components, U1 snRNP and U2AF.

Identifying splicing-related proteins involved in mammalian psychological stress-responses may not only shed light on the molecular mechanism of AChE involvement in stress, but may have an imperative impact on the understanding of gene expression patterns in CNS pathologies in general including chronic stress, post-traumatic stress disorder (PTSD) and other neurodegenerative disorders. Additionally, the levels of various neuromodulators are modified following stress in the prefrontal cortex (PFC), one of the major areas involved in mammalian stress responses.[23] Examples include serotonin,[24] dopamine,[25] acetylcholine[26] and glutamate.[27] Functional implications of such changes involve, for example, impairment of spatial working memory.[28] Therefore, we predicted that changes in the expression of SR-related proteins within the PFC might be a means to adapt to the new situation.

Here, we identified significant and long-lasting overexpression of the splicing factor SC35 weeks after stress. In cotransfection experiments with SC35 and an AChE minigene, SC35 shifted alternative splicing towards the stress-associated variant, AChE-R mRNA. The relationship between SC35 and AChE-R was further demonstrated in the mouse brain after stress and during embryonic development. To our knowledge, this is the first report of the involvement of a splicing factor in mammalian stress responses.

Materials and methods

Adult animals

Naïve FVB/N mice were kept at a 12 h dark/12 h light diurnal schedule and watered/fed *ad libitum*. Stress and corticosterone experiments included two 4-min daily swim sessions or a daily intraperitoneal (i.p.) injection (10 mg/kg) of corticosterone (Sigma, Saint Louis, MO, USA) or saline for 4 consecutive days. Mice were killed 2 weeks thereafter, and brains were dissected on ice and frozen in liquid nitrogen. Blood was collected either from the orbital sinus under halothane (Rhodia, Bristol, UK) anesthesia using an EDTA-containing capillary, or, upon decapitation, directly from the aorta into EDTA-containing centrifuge tubes. Corticosterone levels were determined by radioimmunoassay (Coat-A-Count, DPC, Los Angeles, CA, USA) in plasma separated by slow centrifugation (500 *g*, 30 min, 4°C).

Embryos

CD1 mice were kept at a 12 h dark/12 h light diurnal schedule and watered/fed *ad libitum*. Females were mated by housing with a male mouse overnight and examined the next morning for the presence of vaginal plugs to indicate conception, which was designated embryonic day (E) 0. Embryos at E11, 13 and 15 were collected for this study. At 3 min prior to killing, pregnant dams were deeply anesthetized by an intramuscular injection of a ketamine (50 mg/kg) and xylazine (10 mg/kg) mixture. Embryos were quickly removed from the dams by hysterectomy, transferred to ice cold phosphate-buffered saline (PBS), and the embryonic sac was removed. Embryonic age was verified by measuring crown-rump length (CRL), and only embryos that exhibited close to average CRL values were employed. The embryos were decapitated and whole heads were immersed in 4% paraformaldehyde in PBS for 48 h at 4°C, dehydrated in alcohol and embedded in paraffin. Coronal 4 μm sections through the developing somatosensory cortex were collected by adhesion to Superfrost®-Plus slides (Menzel-Glaser, Braunschweig, Germany).

Cells

COS-1 or human embryonic kidney (HEK) 293 cells were grown in six-well plates in a humidified atmosphere in Dulbecco's modified Eagle's medium (DMEM, Biological Industries) supplemented with 10% fetal calf serum (FCS) and 2 mM L-glutamine at 37°C, 5% CO_2. DNA transfections were carried out using Lipofectamine-Plus (Gibco BRL Life Technologies, Bethesda, MD, USA) with 1 μg plasmid DNA per well as instructed. At 24 h post-transfections, cells were harvested with RNA-Later reagent (Ambion, Austin, TX, USA) and RNA was extracted using RNeasy Mini Kit (Qiagen, Hilden, Germany) and diluted to 100 ng/μl.

Real-time RT-PCR

LightCycler (Roche Diagnostics, Basel, Switzerland) equipped with dedicated software (ver. 3.5) was used to amplify 200 ng samples of RNA template (SYBR Green I RNA amplification kit, Roche). Primers (Sigma, Jerusalem, Israel) used in this study are shown in Table 1. In all experiments, values were normalized to actin mRNA, which remained unchanged. Samples that displayed deviated levels of actin mRNA by 1.5 or more were discarded.

In situ *hybridization*

Paraffin-embedded horizontal whole-brain sections of stressed and control mice were used, essentially as described.[13] Synthetic 2′-*O*-methyl 5′-biotin-labeled RNA probe (Microsynth, Balgach, Switzerland) for SC35 was as described.[29] For ASF/SF2, the probe 5′-TGCGACUCCUGCUGUUGCUUCUGCUACGGCUUCU GCUACGACUACGGCUU-3′ was designed using Oligo software (Molecular Biology Insights, Cascade, CO, USA). Streptavidin–fluorescein conjugate diluted 1 : 100, an anti-AP converter and Fast Red substrate (all from Roche Diagnostics), were used for detection. Paraffin-embedded sections of embryonic brains were similarly processed, applying streptavidin–Cy5 conjugate for detection of biotinylated probes directed to AChE-R mRNA, and antidigoxygenin–Cy3 conjugate for detection of digoxygenin-labeled probes directed to AChE-S mRNA (Jackson ImmunoResearch Laboratories, Cambridgeshire, UK).

Immunohistochemistry

Paraffin sections were deparaffinized with xylene, rehydrated in graded ethanol solutions and DDW, and incubated for 5 min in PBS. For antigen retrieval, slides were heated in a microwave oven at maximal power (850 W, 10 min) in 500 ml of 0.01 M citric buffer, pH 6.0, cooled for 5 min, and rinsed with PBS. Sections were incubated with anti-SC35 (Sigma; diluted to 1 : 50 in PBS with 0.5% Tween-20, 1.5 h, room temp.). Following a rinse with PBS and incubation with biotinylated anti-mouse IgG (Vector Laboratories, Burlingame, CA, USA; diluted 1 : 200 in PBS with 0.5% Tween-20, 1 h, room temp.), sections were rinsed with PBS and incubated with avidin-bound peroxidase complex (ABC Elite kit, Vector Laboratories, 1 h, room temp.) or Cy3-conjugated streptavidin (Jackson Immunoresearch). After rinsing with 0.05 M Tris pH 7.6, the peroxidase was reacted for 90 s with 0.05% diaminobenzidine (Sigma) supplemented with 0.05% nickel ammonium sulfate and 0.006% H_2O_2 in 0.05 M Tris pH 7.6 for color intensification. The color reaction was terminated by rinsing with PBS, sections were dehydrated in ascending concentrations of alcohol, cleared in xylene and covered with Eukitt (Calibrated Instruments, Hawthorne, NY, USA).

Table 1 Primer sequences used in this study

Gene	*Accession #*	*Forward primer*	*Position*	*Reverse primer*	*Position*
SRp20	Z85986	GCCGTGTAAGAGTGGA	374–389	AAGGGCTAGTTGACTGG	540–556
SRp30c	U30825	CAGTGTCGGCTTCGTGTGGA	287–306	AGACCGAGACCGTGAGTAGC	624–643
SRp40	U30826	CGAGGTGGAAGAGGTAGAGG	318–337	GGCACGGGAGACCTACTAAC	777–796
SRp55	U30883	CGGATGCCCACAAGGAACGA	521–540	ACCTGGAACGGGAGCGACTT	768–787
SF2p32	L04636	GAATGGGACAGAAGCGA	417–433	GTGGTCATATAAGGCCCAG	774–792
U5-100	AF026402	CAGCGTCAGGCAATTC	1291–1306	CCTAGCGGTTTCCCAA	1511–1526
9G8	L22253	GGCGCTGGCAAAGGAGAGTT	166–185	CGGCTGCTTCTTGGTCGTGA	715–724
SC35	AF250135	TCCAAGTCCAAGTCCTCCTC	31–50	ACTGCTCCCTCTTCTTCTGG	163–182
ASF/SF2	M69040	TCGAGTCCGCGCTTTTCG	99–117	GCTTCGAGGAAACTCCAC	380–397
p54	NM_004768	TCTTCTGCCTGGTGGTGGAC	482–501	GGGATGGTGAGCGGGACAAT	1175–1194
hnRNPA1	NM_002136	AAAGTCTCTCTTCACCCTGC	81–100	AAGTGGGCACCTGGTCTTTG	390–409
AChE-S	AF002993	CTTCTGGAACCGCTTCCTCCCCAAATT	7855–7881	GTAGTGGTCGAACTGGTTCTTCCAGTGCAC	6916–6945
AChE-R	AF002993	CTTCTGGAACCGCTTCCTCCCCAAATT	7855–7881	GGTTACACCTGGCGGGCTCC	7779–7798
mβ-actin	X03672	CAATTCCATCATGAAGTGTGAC	917–938	ATCTTGATCTTCATGGTGCT	1047–1066
hβ-actin	AJ251794/5	CACTCTTCCAGCCTTCCTTCC	1–21	CGGACTCGTCATACTCCTGCTT	1–22

Standard curves were produced for each primer set using four different dilutions (two-, four-, eight- or 16-fold) of template RNA or cDNA as described.[59]

Structural modeling
The RRM domains of SC35 and ASF/SF2 were modeled using SWISS-MODEL[30] and were superimposed using Deep View spdbv 3.7.

Results

Long-lasting cooverexpression of SC35 and AChE following stress
To search for splicing factors that might mediate stress-induced changes in neuronal long-lasting alternative splicing, we subjected FVB/N mice to 4 consecutive days of repeated swim sessions (2×4 min) and killed them 2 weeks later.[13] Orbital sinus blood of stressed mice served to quantify corticosterone levels following the second swim session as compared with naïve, nonstressed mice. Plasma corticosterone levels rose by ca. five-fold following stress (from 50 ± 13 to 259 ± 53 ng/ml, $P<0.05$, two-tailed Student's *t*-test, Figure 1a), and receded to close to normal levels (76 ± 25, $P>0.1$) 2 weeks later. In comparison, we subjected mice to repeated corticosterone (i.p., 10 mg/kg) or saline injections. Plasma corticosterone rose by ca. four- and two-fold and receded to normal levels 2 weeks later (Figure 1a), demonstrating the peripherally transient nature of both these hormone and stress effects.

Using RNA extracted from the PFC of poststress as compared to hormone-treated or naïve brains, we tested the expression level of several abundant SR-related transcripts. Real-time RT-PCR quantification involved SRp20, SRp30c, SRp40, SRp55, p54, 9G8, ASF/SF2 and SC35, as well as hnRNP A1, the U5-100 kDa and the 32 kDa subunit of SF2, SF2p32. Most of the splicing factors tested did not display any long-lasting stress-induced expression difference (Figure 1b). Exceptions were SC35 and U5-100 kDa, both of which displayed significant sustained overexpression ($P<0.05$, Kruskal–Wallis test, Figure 1b). In addition, 9G8 showed a slight, nonsignificant downregulation, and p54 and SF2p32 displayed nonsignificant upregulation. Neither saline nor corticosterone induced such changes in PFC mRNAs (Figure 1b), suggesting that the observed changes reflected a genuine long-lasting stress response.

To test whether the stress-associated increases in SC35 mRNA levels would occur in cultured cells as well, we subjected COS-1 and HEK-293 cells to a variety of different stressors: UV (germicidal 254-nm UV lamp, 2 J/m^2/s, 30 s), H_2O_2 (500 μM), sorbitol (600 mM), dexamethasone (10 μM) and cortisol (10 μM). Cells were harvested 6 h following treatments, total mRNA was extracted and subjected to real-time RT-PCR analyses using primers for SC35 and β-actin. No change was found in the mRNA levels for SC35 in all of the different treatments (Figure 1c).

SC35 shifts AChE's alternative splicing towards AChE-R in transfected cells
The long-lasting association between AChE-R and SC35 poststress increases could be either direct or

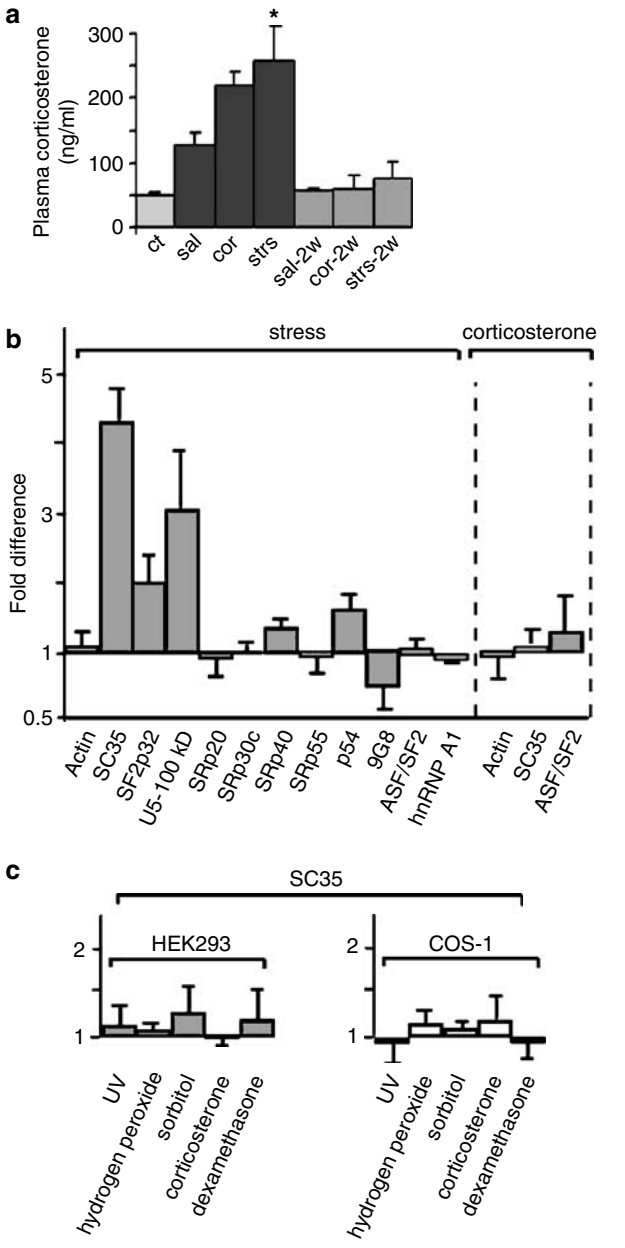

Figure 1 Prefrontal cortex following repeated organismal stress display long-term SC35 overexpression. (a) Plasma corticosterone levels in control (ct, $n=4$), saline-injected (sal, $n=3$), corticosterone-injected (cor, $n=4$) and stressed mice (4 left columns, $n=4$) and 2 weeks later (2w, right columns). (b) mRNA expression levels for a selection of splicing-related factors using real-time RT-PCR on RNA extracted from mouse prefrontal cortex 2 weeks following repeated stress (stress, $n=4$) or 2 weeks following repeated corticosterone injections (corticosterone, $n=4$). β-Actin (left, $n=4$) was used as control. (c) SC35 mRNA expression level following different cellular stressors in HEK293 (left, $n=8$) and COS-1 (right, $n=8$) cells. When animals were used, the given value is an average of at least three different measurements $\pm$ standard deviations from three or more different animals. Asterisks note statistically significant differences from control ($P<0.05$, Kruskal–Wallis test).

indirect. To distinguish between these possibilities, we scanned the AChE pre-mRNA sequence for ESE and ISE. To focus on potentially relevant sequences, we selected only those that were present in both the human and mouse *ACHE* genes. Selected sequences include motifs for the splicing factors SC35, ASF/SF2 and SRp20 in the 3′ alternative splicing-prone region of both human and mouse pre-mRNAs (Figure 2a). These can potentially serve both as ESEs or ESS. The SC35 and SRp20 motifs are found within the intron between exons 5 and 6, whereas the ASF/SF2 motif appears in exon 6.

To test for causal relationships, we examined the influence of SC35, ASF/SF2 and SRp20 on the splicing pattern of an *ACHE*-minigene construct, offering two 3′ splice options[31] (Figure 2b). SC35, ASF/SF2 or SRp20 were cotransfected with the ACHE-minigene into COS-1 or HEK293 cells, both of which possess low levels of endogenous AChE activity.[32]

The CMV promoter was reported to generate primarily 'readthrough' transcripts, for example, when inserted in front of the EDI minigene.[33] Compatible with this tendency, when the CMV-*ACHE* minigene was cotransfected together with an insert-free plasmid or a GFP plasmid, much of the mRNA that was generated was of the readthrough form, AChE-R. Cotransfections with SC35 further elevated AChE-R mRNA levels in a dose-dependent manner, reflecting avoidance of the splice site between E4 and I4. Parallel slightly reduced AChE-S mRNA levels indicated suppressed efficacy of the splicing event linking E4 with E6. Together, this induced a change of over five-fold in the R/S ratio (Figure 2c, d, $P<0.05$, Kruskal–Wallis test). In contrast, cotransfections with ASF/SF2 shifted splicing towards the AChE-S form, however, in a much more variable manner. Finally, cotransfection of the *ACHE* minigene with the SR protein SRp20 showed no apparent change in the AChE-R/AChE-S splicing ratio (Figure 2). There was no detectable contribution of unprocessed RNA to our measured AChE-R levels, since both reactions with no RT, and cell lines that produce only AChE-S yielded

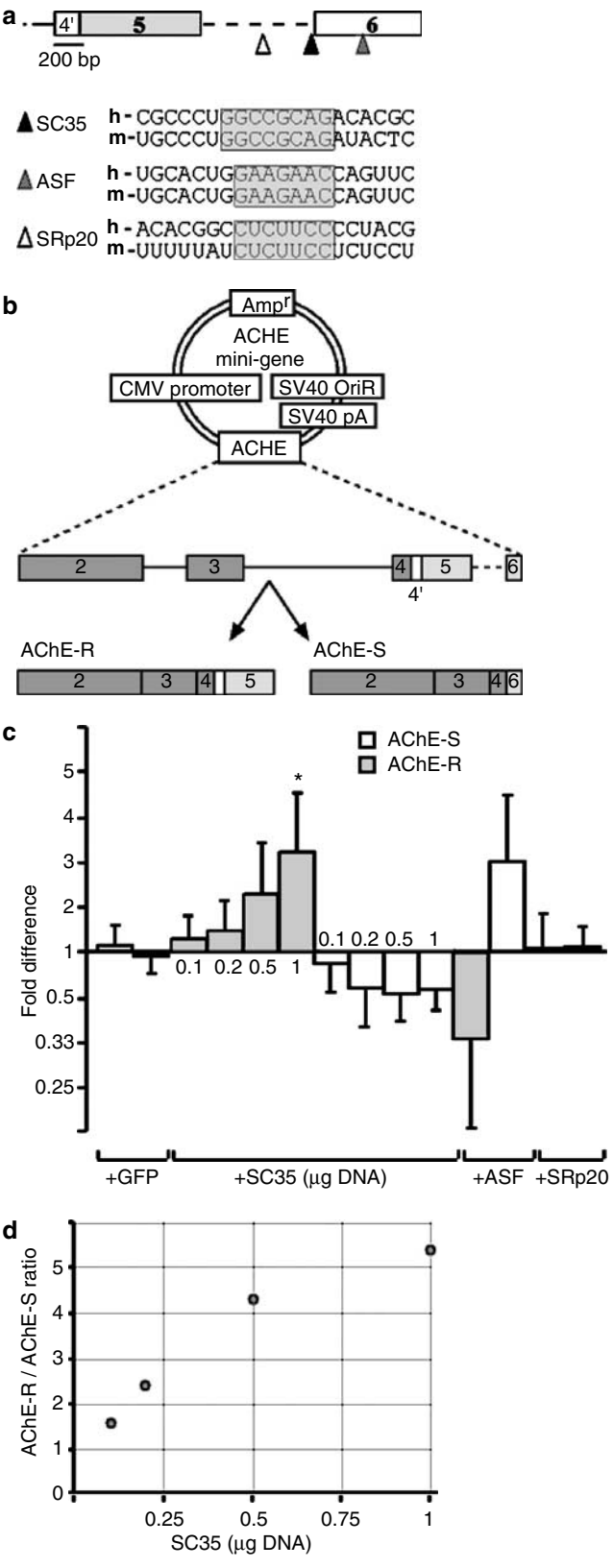

Figure 2 Transfected SC35 shifts alternative splicing towards AChE-R mRNA. (a) Putative splicing factor binding sites on the 3′ region of AChE pre-mRNA. Consensus sequences identified for SC35, ASF/SF2 and SRp20 in human (h) and mouse (m) AChE pre-mRNA are shown. Triangles note their position on the AChE primary transcript. (b) Schematic diagram of the AChE minigene used in a cotransfection assay. Ampicillin resistance (Amp^r), CMV promoter, SV40 origin (OriR) and polyadenylation (pA) sites and the AChE genomic DNA insert spanning the entire coding sequence, from exon 2 to exon 6, including all introns are noted. This insert allows production of either AChE-S or AChE-R transcripts, shown below. (c) Real-time RT-PCR analysis of cotransfection of the AChE mini-gene with SRp20, SC35 and ASF/SF2. Cotransfected GFP served as negative control (left). Columns show fold difference from control for AChE-R and AChE-S mRNA. SC35 was transfected in a concentration-dependent manner. Numbers represent μg plasmid transfected. Asterisk notes $P<0.05$ (Kruskal–Wallis test, $n=8$). (d) AChE-R/AChE-S mRNA ratio as a function of μg SC35 transfected.

no AChE-R product (see Figure 3 below and data not shown).

SC35 is composed of a single N-terminal RRM and a single C-terminal RS domain, whereas ASF/SF2 includes two RRMs and a single RS domain (Figure 3a). In principle, the splice shift promoted by SC35 could be directly due to the RRM. Alternatively, indirect interactions of the RS domain with other proteins could be the cause. In addition, excess SC35 could compete with the splice site selection effects of ASF/SF2.[34,35] To study the effect of specific SC35 and ASF/SF2 elements on the endogenous AChE mRNA splicing of host cells, we conducted single transfection experiments with different constructs carrying various combinations of the RRM and RS domains of SC35 and ASF/SF2 (Figure 3a). AChE-R mRNA is undetectable in control cells; therefore, we measured AChE-S mRNA.

When SC35 was transfected alone (construct I), when ASF/SF2 and SC35 were fused (construct II), or when a construct composed of SC35 RRM and ASF/SF2 RS domains (construct III) was transfected, AChE-S mRNA was reduced (Figure 3b). However, cotransfections where the two RRMs of ASF/SF2 were present without the RRM of SC35 (Figure 3b, constructs IV–VI) induced AChE-S mRNA elevation ($P<0.05$ for constructs I, II, IV and V; $P<0.07$ for constructs III and VI, Kruskal–Wallis test). As SC35 exerts a stronger influence on AChE's splicing pattern, this finding is compatible with the assumption that the SC35 RRM was the cause. This also suggests that in the presence of the SC35 RRM, the opposing ASF/SF2 effect on AChE splicing is minor. A comparison of the mouse SC35 RRM with ASF/SF2 RRM1 (Figure 3c) shows strong ($\sim$50%) sequence similarity, but the calculated pIs for these domains are significantly different, being 8.3 and 4.7 respectively. Even when both ASF/SF2 RRMs are taken into account, their pI together only reaches 7.7. In addition to the differences in the sequences themselves, pI differences may also account for distinct regulatory activity of each splicing factor. Thus, SC35, with a positively charged RRM, promoted the 'readthrough' option of 3′ AChE splicing.

Elevated SC35 mRNA and nuclear SC35 accumulation in poststress prefrontal cortical neurons

The poststress RT-PCR analyses pointed at SC35 increases as potentially associated with the long-lasting changes in neuronal mRNA splice patterns. This predicted direct interaction between neuronal SC35 expression and the 3′ splicing events forming AChE-R mRNA (Figure 4a).[13] In addition, previous tests in our laboratory demonstrated association of the primary AChE-S mRNA transcript with ASF/SF2.[36] Therefore, we explored possible association of neuronal SC35 and ASF/SF2 with AChE alternative splicing *in vivo*. Using *in situ* hybridization on paraffin-embedded brain sections, we observed similarly intense ASF/SF2 labeling throughout the deep layers of the PFC in both naïve (left) and poststress (right) brain (Figure 4b). SC35 mRNA, however, appeared to be relatively scarce in the naïve brain. In contrast, part of the deep layer neurons became SC35 mRNA-positive in the poststress brain (Figure 4c). Immunohistochemical staining revealed corresponding stress-induced increases in nuclear SC35 accumulation at the protein level, within neuron-enriched cell layers (Figure 4d).

In parallel, we studied the AChE splice variants in the PFC. Similar to what we previously observed in the hippocampus,[13] AChE-S mRNA maintained constant levels (Figure 4e), while neuronal AChE-R mRNA was virtually undetectable in the naïve state, but became pronounced in the poststress brain (Figure 4f). Hematoxylin–eosin staining and neuronal cell counts suggested that large fractions of the deep-layer neurons were positive for ASF/SF2 (Figure 4g, h) as well as for AChE-S mRNAs (14 ± 3 and 12.5 ± 3 cells per $100\,\mu m^2$, Figure 4b and e, respectively). Similar fractions of the PFC neurons further expressed elevated SC35 and splice-shifted AChE-R

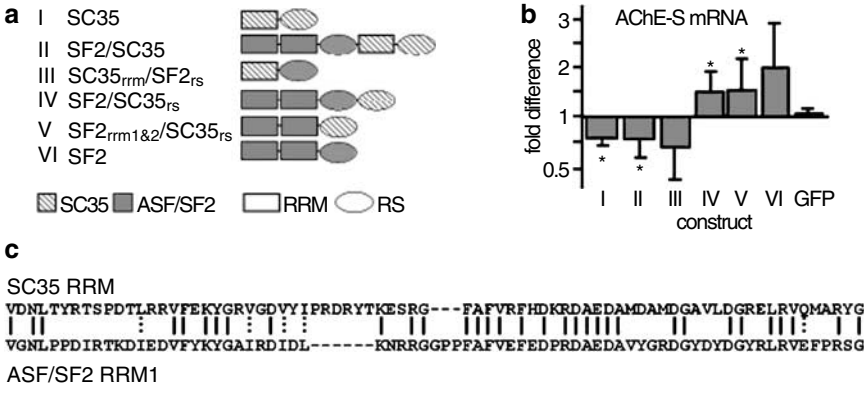

Figure 3 Splicing of host cell AChE by SC35 and ASF/SF2 domains. (a) Different fusion constructs (I–VI) used are shown, which carry the RRM or RS domains of either SC35 or ASF/SF2. (b) Host cells AChE-S mRNA levels (fold difference from control) detected by real-time RT-PCR. Asterisk notes $P<0.05$ (Kruskal–Wallis test, $n=6$). (c) Alignment of SC35 RRM (top) and ASF/SF2 RRM1 (bottom). The two RRMs share some 50% similarity.

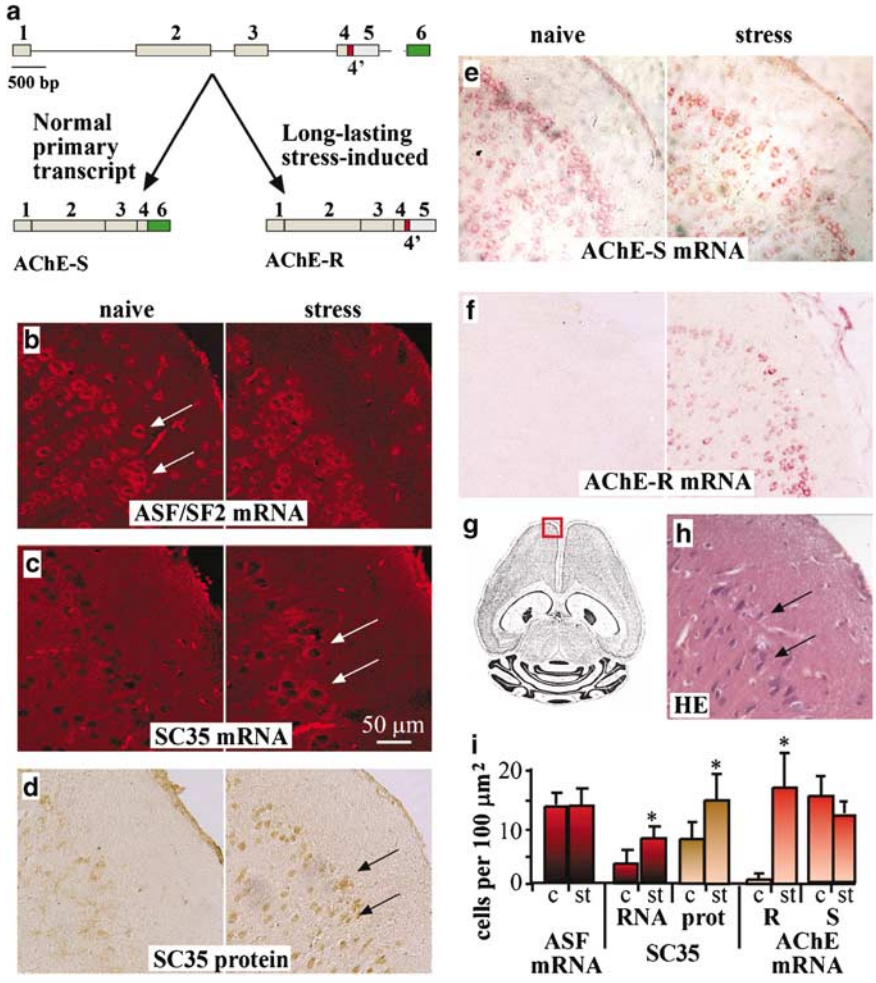

Figure 4 Stress-induced SC35 overexpression in prefrontal cortical neurons. (a) *ACHE* gene structure (top) and neuronal 3′ alternatively spliced products (bottom). (b–c) Fluorescent *in situ* hybridization for ASF/SF2 (b) and SC35 (c) mRNAs. Confocal images shown are series projections. Positively labeled cytoplasms for ASF/SF2 mRNA is stained red (arrows) in both naïve (b, left) and stressed (right) mice. SC35 was difficult to detect in naïve brains (c, left) but was notably overexpressed following stress (right). (d) Immunohistochemistry using monoclonal anti-SC35 antibody. Note the faint nuclear labeling of naïve brain (left) as compared to the intense poststress labeling (right, arrows). (e–f) Fluorescent *in situ* hybridization for AChE-R (e) and AChE-S (f) mRNAs. AChE-R displayed marked overexpression in the prefrontal cortex 2 weeks following stress, while AChE-S remained unchanged. (g) Schematic diagram of a horizontal mouse brain section. The rectangle shows the area of the images taken. (h) Hematoxylin–eosin staining shows tissue morphology. Nuclei are labeled dark purple (arrows). (i) Cell counts per 100 square microns in control (c) and stressed (st) tissues. Fluorescent measurements were as described.[13] Asterisks note significant differences ($P<0.005$, two-talied Student's *t*-test. Values represent counts from at least 40 cells from at least three different animals).

mRNA following stress (15 ± 4 and 17 ± 6 cells per $100\,\mu m^2$, respectively), with parallel increases at the SC35 protein level (Figure 4i). Together, this suggests a stress-induced change from AChE-S mRNA, characteristic of the naïve brain to an SC35-AChE-R mRNA association in the poststress PFC.

Transient SC35 overexpression coincides with AChE-R/AChE-S dominance in the developing brain

Maternal stress during pregnancy was reported to cause long-lasting deleterious effects in the offspring,[6] suggesting that stress affects brain development. Also, we have recently shown that neuronal progenitor cells express both AChE-S and AChE-R, which exert distinct effects on cortical development.[37] To explore the possibility that SC35–AChE interactions are involved, the developing mouse cortex was subjected to comparative *in situ* hybridization and immunohistochemistry analyses.

Excitatory neurons in the cerebral neocortex emerge from a pseudostratified neuroepithelium in the ventricular zone (VZ) that lines the ventricular cavity of the developing cerebral wall.[38] The postmitotic neurons that are generated migrate away from the VZ to reach the outer surface of the cortical wall and subsequently differentiate in the developing cortical

plate (Figure 5a). In the murine embryonic brain, immunohistochemistry demonstrated labeling of the SC35 protein primarily in round nuclei of cells adjacent to the ventricular lumen, where DNA replication occurs, that is, during mitosis of the neuroepithelial cells (Figure 5b). At the onset of neurogenesis (E11), the AChE-R and AChE-S mRNA variants colocalized, intensively expressed in the cytoplasm of the majority of neuroepithelial cells born in the VZ, as shown by *in situ* hybridization (Figure 5c). At E13, AChE-S mRNA labeling exhibited a significant decrease ($P<0.01$, two-tailed Student's *t*-test), while AChE-R mRNA labeling remained relatively unchanged, yielding an elevated AChE-R/AChE-S ratio. The AChE-R transcript decreased later, at E15 ($P<0.001$), becoming coleveled again with AChE-S. The number of SC35 expressing cells increased by 31% at E13 but declined back by 57% at E15 (Figure 5d). At this time period, AChE-S mRNA expression levels were downregulated with the advance of neurogenesis, to 59 and 46% of the level at E11. The reduction in AChE-R mRNA was more abrupt, down to 95% at E13 and 37% at E15 (Figure 5d), suggesting causal association in this modified AChE-R/AChE-S ratio of the splicing factor SC35 and its target AChE pre-mRNA during neurogenesis.

SC35 overexpression in AChE-R transgenic mice

SC35 exerts an autoregulatory, alternative splicing mediated, control over its own mRNA levels.[39] The long-term SC35 overexpression following stress therefore raised the question whether changes in cholinergic neurotransmission, such as those occurring under long-term stress reactions, may modify the SC35 level maintained by this mode of control. To challenge this hypothesis, we explored SC35 expression in transgenic animals constitutively overexpressing neuronal AChE-S or AChE-R. Mice overexpressing the synaptic human AChE-S (TgS mice) show accelerated stress-related pathology and neuromuscular malfunctions,[12,40] whereas AChE-R-expressing mice (TgR) display normal neuromuscular function and their brains are relatively protected from the stress-associated hallmarks of pathology.[12] SC35 immunohistochemistry was carried out on 10-μm-thick paraffin-embedded coronal sections (Figure 6a, b) of FVB/N controls (Figure 6c), TgS (Figure 6d) and TgR (Figure 6e) mice, and fluorescence intensity in the labeled nuclei was measured in the motor and prefrontal cortices. In the stress-prone TgS mice, the population distribution of neuronal SC35 levels was comparable to that of strain-matched FVB/N controls (wt). In contrast, in the stress-protected TgR mice, larger fractions of cortical neurons presented high

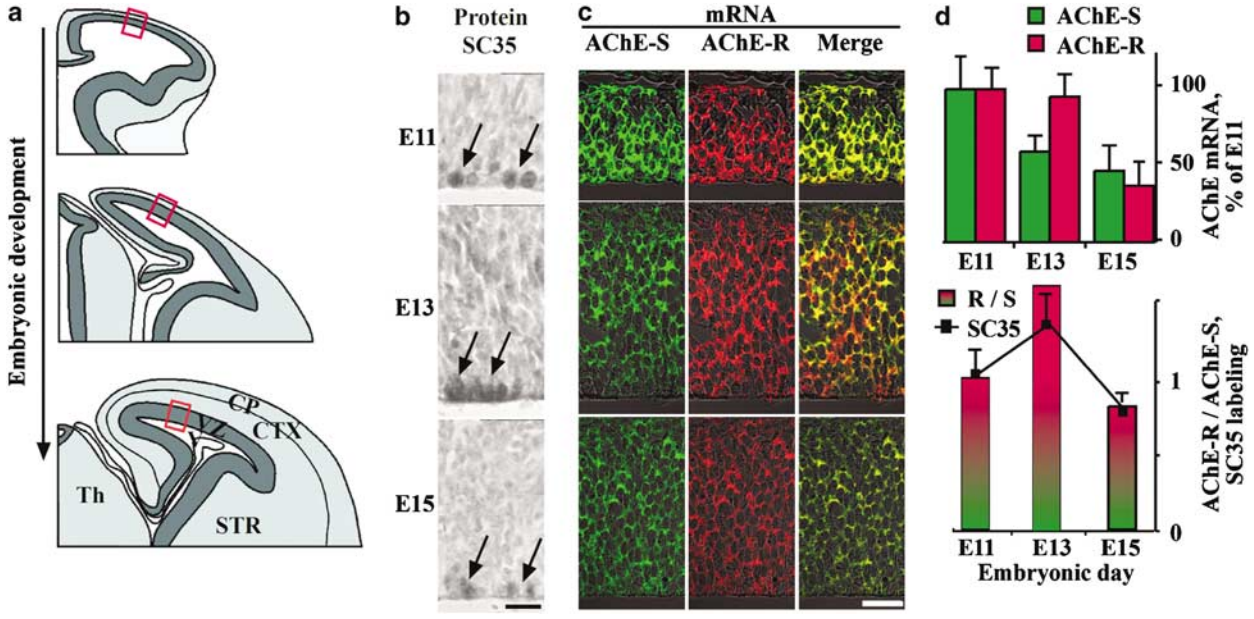

Figure 5 Transient dominance of AChE-R over AChE-S mRNA correlates with increased expression of SC35 during brain development. (a) Schematic diagram of the developing cortex, from top to bottom, at embryonic days (E) 11, 13 and 15. Rectangles represent the areas of the images taken. STR, striatum; CTX, cortex (somato-sensory); CP, cortical plate; VZ, ventricular zone; V, ventricle; Th, thalamus. (b) Immunolabeling of SC35 protein (grayscale). Arrows point to mitotic cells expressing SC35. (c) Confocal images showing *in situ* hybridization labeling of AChE-R (Cy5, red pseudocolor) and AChE-S mRNA (Cy3, green pseudocolor) during cortical development (from E11, top to E15, bottom). Merged figures demonstrate the colocalization of the AChE transcripts at E11 and E15 as well as AChE-R mRNA dominance at E13. Bars = 25 μm. (d) Quantified intensity of AChE-S (green) and AChE-R (red) mRNA labeling compared to their expression at E11 (top). Ratio between AChE-R and AChE-S mRNA (columns) is compared to changes in SC35 expressing mitotic figures (squares) from E11 (top) to E15 (bottom). For quantification, at least 80 cells were analyzed from at least five different brains. See text for *P*-values.

levels of nuclear SC35 (Figure 6f). Support of this observation comes from an analysis of the distribution of signal densities in neuronal nuclei for all sections analyzed. Although the distributions for FVB/N and TgR cortices overlap broadly, they do differ significantly ($P<0.001$, $F=22.3$, two-way ANOVA). Multiple comparison analysis confirmed that TgR mice are different in a statistically significant manner from TgS or wt mice ($P<0.05$, Bonferroni test). These results suggest that neuronal AChE-R overexpression in the murine brain additionally reinforces an elevation of neuronal expression of SC35 itself.

Discussion

Neuronal PFC expression of the *ACHE* gene provides an appropriate test case for studying the involvement of SR proteins in long-lasting stress responses, because AChE pre-mRNA undergoes a multitude of changes. Others have shown that AChE mRNA levels depend, to a large extent, on the HuD RNA-binding protein.[41] Our present findings add the SR protein SC35, as a key causal element in the maintenance and splicing decisions of neuronal AChE mRNA levels.

The *ex vivo* capacity of SC35 to affect the splicing pattern of AChE was demonstrated in this study in transfected COS-1 and HEK293 cells. Both are easily amenable to transfection and possess extremely low levels of endogenous AChE, which allowed simple interpretation of the results. Our findings that SC35 and AChE-R mRNA levels appear to be directly interrelated in the stressed adult brain, the developing mouse brain and the brain of TgR transgenic mice support the theory that SC35 influences AChE

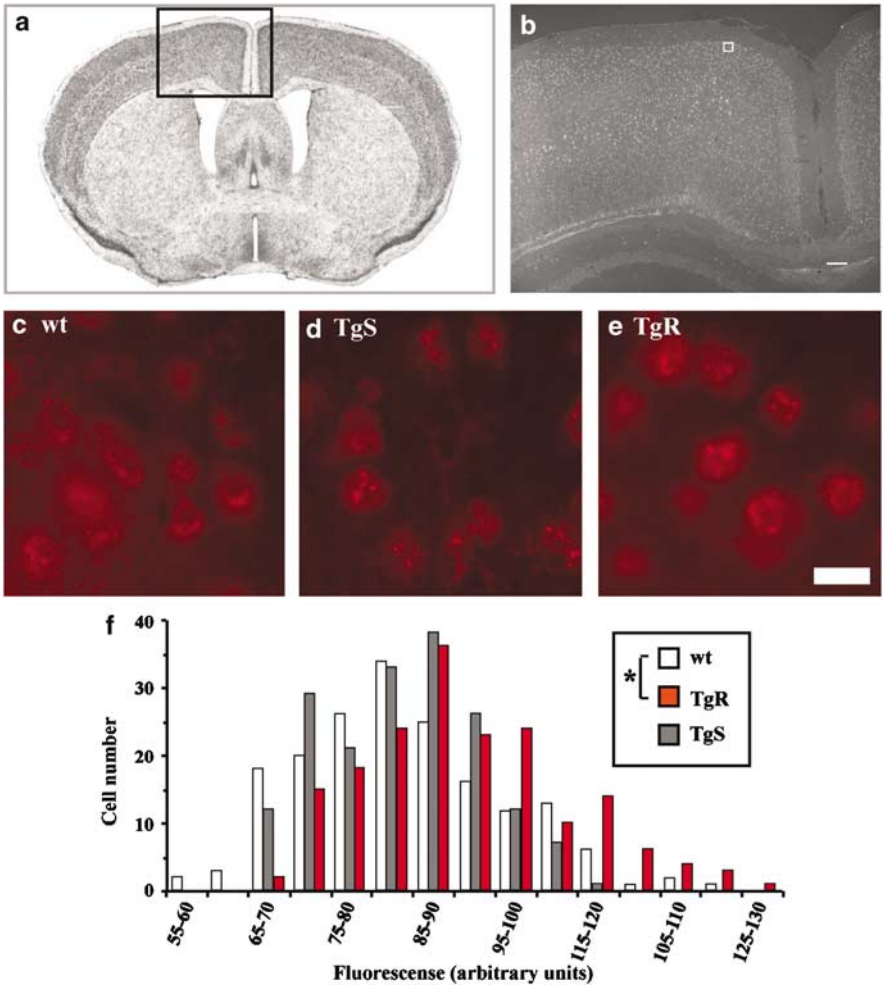

Figure 6 Elevated SC35 levels in TgR mice. (a) Coronal mouse brain section depicting the area analyzed in this experiment. (b) Immunohistochemistry for SC35 was conducted on paraffin-embedded brain sections (boxed area in (a)) from adult age- and gender-matched mice of the noted strains. Bar = 100 μm. (c) SC35 immunostaining in wt FVB/N mice. (d) SC35 in TgS mice. (e) SC35 in TgR mice. Bar = 10 μm. (f) Distribution of fluorescence density (arbitrary units) in wt (empty bars), TgS (gray bars) and TgR (red bars) mice. Values represent $n=180$ cells from six different animals of each strain. Note that cortical neurons from TgR, but not TgS mice, include larger fractions of cells with intensive SC35 labeling as compared to wild-type FVB/N controls. Asterisk notes $P<0.005$, two-way ANOVA.

pre-mRNA splicing in the same manner in neurons, and that AChE-R excess reciprocally elevates neuronal SC35 levels.

Comparison, using real-time RT-PCR, of AChE mRNA levels in the PFC of naïve, saline- and corticosterone-injected or psychologically stressed mice showed that stress, but not repeated injections of saline or corticosterone, induced long-lasting changes in neuronal SC35 expression. Thus, the initial activation of the HPA axis appears insufficient to turn on and maintain the long-term stress-induced changes in neuronal SC35 expression. That cortisol or dexamethasone treatment failed to induce SC35 overexpression in cultured cells supports this notion. SC35 was, however, markedly overexpressed in the stressed brain for at least 2 weeks and shifted, in cultured cells, the alternative splicing of the *ACHE* mini-gene towards AChE-R mRNA. Correspondingly, expression of SC35 at the mitotic phase of progenitor cells paralleled a transient dominance of AChE-R over AChE-S expression during murine cortical development. As SC35 expression declined, the AChE-R dominance faded, further suggesting a relationship between the two. Reciprocally, transgenic AChE-R dominance in adult mice induced chronic neuronal SC35 elevation, indicating a reinforcement mechanism whereby SC35 supports overproduction of AChE-R and *vice versa*.

Splicing-related proteins in general, and SC35 in particular, may play a central role in mammalian stress responses. By controlling and modifying the expression patterns of stress-related proteins as an adaptation strategy, they can modify relevant transcripts from their usually expressed forms to specially adapted ones.[4] The PFC long-lasting overexpression of SC35 in close association to that of AChE-R is consistent with this hypothesis. SC35 is also intensively expressed in the developing neocortex, primarily in progenitor cells as they pass through the mitotic phase of the cell cycle and express AChE-R. Prolonged overexpression of SC35 and the morphogenic AChE-R protein,[12] as would be the case under prenatal stress, may possibly impair cortical development, compromising cognitive performance. While additional, yet nonidentified, splicing-related proteins are likely involved (eg Tra2-β1),[21] the contribution of SC35 appears to be pivotal for changes in cholinergic neurotransmission.

As a member of the SR protein family, SC35 possesses both an RRM and an RS domain, and affects both splice site selection and alternative splicing.[42] SC35 further promotes splicing events that destabilize its own mRNA, exercising a self-control mechanism that limits its durability.[39] This, in turn, raised the question of how SC35 mRNA maintains its long-lasting high levels in the poststress brain. A plausible explanation is that the balance between SC35 production and SC35 mRNA alternative splicing and/or degradation might be subject to cholinergic regulation. In this case, the increases in SC35 levels would not be due to the cholinergic hyperexcitation, which accompanies the initiation of stress reactions. Rather, its sustainable excess would reciprocally be due to cholinergic down-tuning and prolonged AChE-R excess (as is the case in TgR transgenic mice). Further studies would be required to characterize a wider profile of splicing regulators in the TgR brain and find out if this profile is modified in this animal model.

An additional splicing-related factor that showed a more moderate overexpression was SF2p32, the 32 kDa subunit of the splicing factor ASF/SF2. ASF/SF2 was also shown to affect both alternative splicing and choice of splice sites.[43] Interestingly, ASF/SF2 also antagonizes SC35 activity in other target sequences.[34,44] In addition, SF2p32 was shown to inhibit ASF/SF2 activity.[45] Thus, elevation of SF2p32 should reduce ASF/SF2 activity even under conditions of unchanged ASF/SF2 levels such as the poststress PFC, where SF2p32 mRNA was slightly elevated, and ASF/SF2 slightly reduced. Although not significant, these changes are compatible with the assumption of suppressed ASF/SF2 activity under long-term stress responses.

The antagonized ASF/SF2 and SC35 activities lead us to structurally compare between the RRMs of these

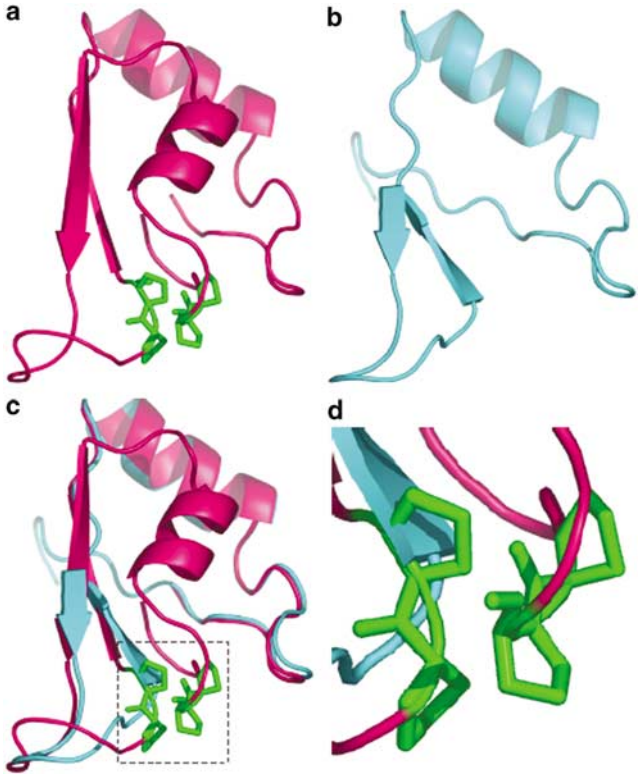

Figure 7 Molecular modeling of SC35 and ASF/SF2 structures. (a) Molecular modeling of ASF/SF2 structure. (b) Molecular modeling of SC35 structure. (c) Superimposition of ASF/SF2 (red) and SC35 (blue) structures. Note the strong similarity, with the exception of the four prolines cluster (green). (d) Enlargement of the proline cluster of ASF/SF2, shown as dashed square in panel c.

two splicing factors. Molecular modeling showed that ASF/SF2 (Figure 7a), but not SC35 (Figure 7b), includes a cluster of four proline residues that are positioned close to each other in the extended region protruding from this RRM domain (Figure 7c, d). Polyproline segments that are part of RRMs are known in other splicing factors, where they were proposed to serve as protein–protein interaction motifs during spliceosome assembly.[46] Our current study raises the possibility that the proline-rich domain in ASF/SF2 contributes toward the dynamic equilibrium balancing between AChE-R and AChE-S, possibly by facilitating ASF/SF2 interactions with other spliceosomal components. The determining factor is hence SC35 regulation, which by changing SC35 levels may tilt this balance towards overproduction of AChE-R.

The mechanisms by which stress initiates the modifications in the composition of splicing-related proteins and the sustained elevation in SC35 is still unknown; however, neuronal activity modulations are likely involved.[47] Acetylcholine levels are notably elevated under stress,[13] and acetylcholine modulates the activity of neurons responding to other neurotransmitters as well (eg glutamate, GABA[48]). Therefore, the capacity to downregulate acetylcholine levels throughout the brain by the soluble AChE-R may be important. In contrast, elevated levels of the synapse-adhered AChE-S would only affect cholinergic circuits, creating an imbalanced cholinergic status. That SC35 levels are elevated in TgR, but not TgS mice, may imply that cholinergic imbalances impair this process.

Apart from SC35 and Tra1β, neuronal stress modifies the subcellular localization of the heteronuclear ribonucleoprotein hnRNP A1 through the MAP kinase cascade, thereby changing alternative splicing patterns.[49] This is especially relevant in our case, as the effects of SC35 and hnRNP A1 usually antagonize each other.[35,50] Other splicing factors, such as SRp30c and ASF/SF2, but not SC35, were shown to be recruited, following cellular stress, to SAM68 nuclear bodies (SNBs).[51] Such recruitment can potentially alleviate competitive interactions of SC35 with its RNA substrates, assisting its function(s). The relocalization of another such protein, hnRNP K, to the cell cytoplasm also depends on the stress-activated ERK MAP-kinase pathway. In activated T lymphocytes, cytoplasmic hnRNP K is involved in the alternative splicing of the transmembrane cell adhesion glycoprotein CD44 by retaining the exon v5 sequence in the mature CD44 mRNA.[52] Normal development of T lymphocytes, which is subject to stress-induced alterations, was shown to depend upon SC35,[42] suggesting that the involvement of SC35 in delayed stress responses extends beyond the nervous system.

Alternative splicing of a growing number of gene products, including AChE, can be found in numerous types of tumors,[53,54] probably reflecting a general modification of the processing machinery during disease state.[2,8] SC35 is overexpressed in a variety of transformed murine cells.[55] In humans, SC35 expression is altered under HIV infection[56] and during pregnancy.[57] ASF/SF2 as well is spatio-temporally regulated in the uterine myometrium during pregnancy,[58] perhaps reflecting a more general phenomenon for the regulation, amenable to therapeutic interference, of splicing-related genes during various stresses or under adaptation to altered conditions.

To conclude, we identified SC35 as a likely factor mediating long-lasting alternative splicing of AChE gene expression in prefrontal cortical neurons following repeated stress and demonstrated close association of SC35 with AChE-R in cultured cells as well as in stressed, developing and transgenic animals.

Acknowledgements

We thank Dr Javier Caceres (Edinburgh) for kindly providing SC35 plasmids and Dr Bat-Sheva Kerem (Jerusalem) for SRp20 and ASF/SF2 plasmids. This study was supported by the Israel Science Fund (618/02-1), the European Union (QLK3-CT-2002-02062, LSHM-CT-2003-503330, DIP-G-3.2) and EURASNET, the Israel–US Binational Industrial Research and Development (BIRD-F) to Ester Neurosciences Ltd (www.esterneuro.com) and Pharmacopeia, Inc. EM has been an incumbent of a Lionel Perez predoctoral fellowship from the Israel Interdisciplinary Center for Neural Computation, the Hebrew University Rector's doctoral fellowship and a Golda Meir fellowship. BB has been an incumbent of a Haselkorn Fellowship. AD has been an incumbent of a postdoctoral fellowship from the Israel Psychobiology Fund.

References

1 Grabowski PJ, Black DL. Alternative RNA splicing in the nervous system. *Prog Neurobiol* 2001; **65**: 289–308.
2 Stamm S, Ben-Ari S, Rafalska I, Tang Y, Zhang Z, Toiber D *et al*. Function of alternative splicing. *Gene* 2005; **344**: 1–20.
3 Dredge BK, Polydorides AD, Darnell RB. The splice of life: alternative splicing and neurological disease. *Nat Rev Neurosci* 2001; **2**: 43–50.
4 Meshorer E, Soreq H. Splicing modulations in senescence. *Aging Cell* 2002; **1**: 10–16.
5 Mitchelmore C, Kjaerulff KM, Pedersen HC, Nielsen JV, Rasmussen TE, Fisker MF *et al*. Characterization of two novel nuclear BTB/POZ domain zinc finger isoforms. Association with differentiation of hippocampal neurons, cerebellar granule cells, and macroglia. *J Biol Chem* 2002; **277**: 7598–7609.
6 Lemaire V, Koehl M, Le Moal M, Abrous DN. Prenatal stress produces learning deficits associated with an inhibition of neurogenesis in the hippocampus. *Proc Natl Acad Sci USA* 2000; **97**: 11032–11037.
7 Nissim-Rafinia M, Kerem B. Splicing regulation as a potential genetic modifier. *Trends Genet* 2002; **18**: 123–127.
8 Stoilov P, Meshorer E, Gencheva M, Glick D, Soreq H, Stamm S. Defects in pre-mRNA processing as causes of and predisposition to diseases. *DNA Cell Biol* 2002; **21**: 803–818.
9 Faustino NA, Cooper TA. Pre-mRNA splicing and human disease. *Genes Dev* 2003; **17**: 419–437.
10 Lin CL, Bristol LA, Jin L, Dykes-Hoberg M, Crawford T, Clawson L *et al*. Aberrant RNA processing in a neurodegenerative disease: the

cause for absent EAAT2, a glutamate transporter, in amyotrophic lateral sclerosis. *Neuron* 1998; **20**: 589–602.
11 Catania MV, Aronica E, Yankaya B, Troost D. Increased expression of neuronal nitric oxide synthase spliced variants in reactive astrocytes of amyotrophic lateral sclerosis human spinal cord. *J Neurosci* 2001; **21**: RC148.
12 Soreq H, Seidman S. Acetylcholinesterase—new roles for an old actor. *Nat Rev Neurosci* 2001; **2**: 294–302.
13 Meshorer E, Erb C, Gazit R, Pavlovsky L, Kaufer D, Friedman A *et al.* Alternative splicing and neuritic mRNA translocation under long-term neuronal hypersensitivity. *Science* 2002; **295**: 508–512.
14 Meshorer E, Toiber D, Zurel D, Sahly I, Dori A, Cagnano E *et al.* Combinatorial complexity of 5′ alternative acetylcholinesterase transcripts and protein products. *J Biol Chem* 2004; **279**: 29740–29751.
15 Tacke R, Manley JL. Determinants of SR protein specificity. *Curr Opin Cell Biol* 1999; **11**: 358–362.
16 Bandziulis RJ, Swanson MS, Dreyfuss G. RNA-binding proteins as developmental regulators. *Genes Dev* 1989; **3**: 431–437.
17 Birney E, Kumar S, Krainer AR. Analysis of the RNA-recognition motif and RS and RGG domains: conservation in metazoan pre-mRNA splicing factors. *Nucleic Acids Res* 1993; **21**: 5803–5816.
18 Cartegni L, Chew SL, Krainer AR. Listening to silence and understanding nonsense: exonic mutations that affect splicing. *Nat Rev Genet* 2002; **3**: 285–298.
19 Hanamura A, Caceres JF, Mayeda A, Franza Jr BR, Krainer AR. Regulated tissue-specific expression of antagonistic pre-mRNA splicing factors. *RNA* 1998; **4**: 430–444.
20 Mintz PJ, Spector DL. Compartmentalization of RNA processing factors within nuclear speckles. *J Struct Biol* 2000; **129**: 241–251.
21 Daoud R, Mies G, Smialowska A, Olah L, Hossmann KA, Stamm S. Ischemia induces a translocation of the splicing factor tra2-beta 1 and changes alternative splicing patterns in the brain. *J Neurosci* 2002; **22**: 5889–5899.
22 Kramer A. The structure and function of proteins involved in mammalian pre-mRNA splicing. *Annu Rev Biochem* 1996; **65**: 367–409.
23 Buijs RM, Van Eden CG. The integration of stress by the hypothalamus, amygdala and prefrontal cortex: balance between the autonomic nervous system and the neuroendocrine system. *Prog Brain Res* 2000; **126**: 117–132.
24 Kawahara H, Yoshida M, Yokoo H, Nishi M, Tanaka M. Psychological stress increases serotonin release in the rat amygdala and prefrontal cortex assessed by *in vivo* microdialysis. *Neurosci Lett* 1993; **162**: 81–84.
25 Hamamura T, Fibiger HC. Enhanced stress-induced dopamine release in the prefrontal cortex of amphetamine-sensitized rats. *Eur J Pharmacol* 1993; **237**: 65–71.
26 Mark GP, Rada PV, Shors TJ. Inescapable stress enhances extracellular acetylcholine in the rat hippocampus and prefrontal cortex but not the nucleus accumbens or amygdala. *Neuroscience* 1996; **74**: 767–774.
27 Bagley J, Moghaddam B. Temporal dynamics of glutamate efflux in the prefrontal cortex and in the hippocampus following repeated stress: effects of pretreatment with saline or diazepam. *Neuroscience* 1997; **77**: 65–73.
28 Mizoguchi K, Yuzurihara M, Ishige A, Sasaki H, Chui DH, Tabira T. Chronic stress induces impairment of spatial working memory because of prefrontal dopaminergic dysfunction. *J Neurosci* 2000; **20**: 1568–1574.
29 Sureau A, Soret J, Guyon C, Gaillard C, Dumon S, Keller M *et al.* Characterization of multiple alternative RNAs resulting from antisense transcription of the PR264/SC35 splicing factor gene. *Nucleic Acids Res* 1997; **25**: 4513–4522.
30 Schwede T, Kopp J, Guex N, Peitsch MC. SWISS-MODEL: an automated protein homology-modeling server. *Nucleic Acids Res* 2003; **31**: 3381–3385.
31 Karpel R, Sternfeld M, Ginzberg D, Guhl E, Graessmann A, Soreq H. Overexpression of alternative human acetylcholinesterase forms modulates process extensions in cultured glioma cells. *J Neurochem* 1996; **66**: 114–123.
32 Velan B, Kronman C, Grosfeld H, Leitner M, Gozes Y, Flashner Y *et al.* Recombinant human acetylcholinesterase is secreted from transiently transfected 293 cells as a soluble globular enzyme. *Cell Mol Neurobiol* 1991; **11**: 143–156.
33 Kadener S, Fededa JP, Rosbash M, Kornblihtt AR. Regulation of alternative splicing by a transcriptional enhancer through RNA pol II elongation. *Proc Natl Acad Sci USA* 2002; **99**: 8185–8190.
34 Gallego ME, Gattoni R, Stevenin J, Marie J, Expert-Bezancon A. The SR splicing factors ASF/SF2 and SC35 have antagonistic effects on intronic enhancer-dependent splicing of the beta-tropomyosin alternative exon 6A. *EMBO J* 1997; **16**: 1772–1784.
35 Expert-Bezancon A, Sureau A, Durosay P, Salesse R, Groeneveld H, Lecaer JP *et al.* hnRNP A1 and the SR proteins ASF/SF2 and SC35 have antagonistic functions in splicing of beta-tropomyosin exon 6B. *J Biol Chem* 2004; **279**: 38249–38259.
36 Lev-Lehman E, Deutsch V, Eldor A, Soreq H. Immature human megakaryocytes produce nuclear-associated acetylcholinesterase. *Blood* 1997; **89**: 3644–3653.
37 Dori A, Cohen J, Silverman WF, Pollack Y, Soreq H. Functional manipulations of acetylcholinesterase splice variants highlight alternative splicing contributions to murine neocortical development. *Cereb Cortex* 2005; **15**: 419–430.
38 Parnavelas JG. The origin and migration of cortical neurones: new vistas. *Trends Neurosci* 2000; **23**: 126–131.
39 Sureau A, Gattoni R, Dooghe Y, Stevenin J, Soret J. SC35 autoregulates its expression by promoting splicing events that destabilize its mRNAs. *EMBO J* 2001; **20**: 1785–1796.
40 Meshorer E, Biton IE, Ben-Shaul Y, Ben-Ari S, Assaf Y, Soreq H *et al.* Chronic cholinergic imbalances promote brain diffusion and transport abnormalities. *FASEB J* 2005; **19**: 910–922.
41 Deschenes-Furry J, Belanger G, Perrone-Bizzozero N, Jasmin BJ. Post-transcriptional regulation of acetylcholinesterase mRNAs in nerve growth factor-treated PC12 cells by the RNA-binding protein HuD. *J Biol Chem* 2003; **278**: 5710–5717.
42 Wang HY, Xu X, Ding JH, Bermingham Jr JR, Fu XD. SC35 plays a role in T cell development and alternative splicing of CD45. *Mol Cell* 2001; **7**: 331–342.
43 Sun Q, Mayeda A, Hampson RK, Krainer AR, Rottman FM. General splicing factor SF2/ASF promotes alternative splicing by binding to an exonic splicing enhancer. *Genes Dev* 1993; **7**: 2598–2608.
44 Caceres JF, Stamm S, Helfman DM, Krainer AR. Regulation of alternative splicing *in vivo* by overexpression of antagonistic splicing factors. *Science* 1994; **265**: 1706–1709.
45 Petersen-Mahrt SK, Estmer C, Ohrmalm C, Matthews DA, Russell WC, Akusjarvi G. The splicing factor-associated protein, p32, regulates RNA splicing by inhibiting ASF/SF2 RNA binding and phosphorylation. *EMBO J* 1999; **18**: 1014–1024.
46 Kielkopf CL, Rodionova NA, Green MR, Burley SK. A novel peptide recognition mode revealed by the X-ray structure of a core U2AF35/U2AF65 heterodimer. *Cell* 2001; **106**: 595–605.
47 West AE, Griffith EC, Greenberg ME. Regulation of transcription factors by neuronal activity. *Nat Rev Neurosci* 2002; **3**: 921–931.
48 Pepeu G, Blandina P. The acetylcholine, GABA, glutamate triangle in the rat forebrain. *J Physiol Paris* 1998; **92**: 351–355.
49 van der Houven van Oordt W, Diaz-Meco MT, Lozano J, Krainer AR, Moscat J, Caceres JF. The MKK(3/6)-p38-signaling cascade alters the subcellular distribution of hnRNP A1 and modulates alternative splicing regulation. *J Cell Biol* 2000; **149**: 307–316.
50 Rooke N, Markovtsov V, Cagavi E, Black DL. Roles for SR proteins and hnRNP A1 in the regulation of c-src exon N1. *Mol Cell Biol* 2003; **23**: 1874–1884.
51 Denegri M, Chiodi I, Corioni M, Cobianchi F, Riva S, Biamonti G. Stress-induced nuclear bodies are sites of accumulation of pre-mRNA processing factors. *Mol Biol Cell* 2001; **12**: 3502–3514.
52 Weg-Remers S, Ponta H, Herrlich P, Konig H. Regulation of alternative pre-mRNA splicing by the ERK MAP-kinase pathway. *EMBO J* 2001; **20**: 4194–4203.
53 Caballero OL, de Souza SJ, Brentani RR, Simpson AJ. Alternative spliced transcripts as cancer markers. *Dis Markers* 2001; **17**: 67–75.
54 Perry C, Sklan EH, Birikh K, Shapira M, Trejo L, Eldor A *et al.* Complex regulation of acetylcholinesterase gene expression in human brain tumors. *Oncogene* 2002; **21**: 8428–8441.

55 Maeda T, Furukawa S. Transformation-associated changes in gene expression of alternative splicing regulatory factors in mouse fibroblast cells. *Oncol Rep* 2001; **8**: 563–566.
56 Maldarelli F, Xiang C, Chamoun G, Zeichner SL. The expression of the essential nuclear splicing factor SC35 is altered by human immunodeficiency virus infection. *Virus Res* 1998; **53**: 39–51.
57 Nie GY, Li Y, Batten L, Griffiths B, Wang J, Findlay JK *et al*. Uterine expression of alternatively spliced mRNAs of mouse splicing factor SC35 during early pregnancy. *Mol Hum Reprod* 2000; **6**: 1131–1139.
58 Pollard AJ, Sparey C, Robson SC, Krainer AR, Europe-Finner GN. Spatio-temporal expression of the trans-acting splicing factors SF2/ASF and heterogeneous ribonuclear proteins A1/A1B in the myometrium of the pregnant human uterus: a molecular mechanism for regulating regional protein isoform expression *in vivo*. *J Clin Endocrinol Metab* 2000; **85**: 1928–1936.
59 Bustin SA. Absolute quantification of mRNA using real-time reverse transcription polymerase chain reaction assays. *J Mol Endocrinol* 2000; **25**: 169–193.